Hardware-in-the-loop heat pump model validation for flexibility evaluations

Maarten Evens [a, b], Alessia Arteconi [a, b, c]

[a] Department of Mechanical Engineering, KU Leuven, 3000, Leuven, Belgium, maarten.evens@kuleuven.be, alessia.arteconi@kuleuven.be

[b] EnergyVille, 3600, Genk, Belgium

[c] Dipartimento di Ingegneria Industriale e Scienze Matematiche, Università Politecnica delle Marche, 60131, Ancona, Italy

Abstract. Heat pumps play a paramount role in carbon emission reductions as they allow the use of sustainable energy. As heat pumps mainly use electricity to provide thermal services, they also enable the provision of energy flexibility services. In this context, new heat pump control strategies are investigated. Though, the comparison of smart and traditional control strategies requires an accurate knowledge of the real heat pump behaviour, both in short- and long-term. Firstly, this paper presents a hardware-in-the-loop set-up which allows a real heat pump behaviour analysis, while the required communication is also shown. Secondly, the test bench was used to validate and further develop a water/water heat pump model. Hence, artificial test cycles were used to distinct and validate the internal control strategies of the heat pump, with the focus on both the short-term behaviour and energy consumption. As the heat pump model started from the manufacturer documentation, comparing the experimental results to the simulations revealed deviated behaviour due to a different modelling approach of the heat pump internal control strategies. Hence, the heat pump model was improved by changing and adding control strategies such as a compressor modulation controller, timing constraints and condenser and evaporator pump control. Although the improved heat pump model reached better profile agreement, deviations remained and indicated a calibration work necessity. Analysis also showed that the real heat pump was not able to quickly recover for the combination of high space heating temperatures and low thermal loads, while increasing the supply temperature for energy flexibility services is common. To conclude, results proved that only using heat pump manufacturer documentation is not sufficient for real heat pump behaviour representation.

Keywords. Heat pump, model validation, hardware-in-the-loop, energy flexibility.
DOI: https://doi.org/10.34641/clima.2022.242

1. Introduction

Heat pumps (HP) can play a paramount role to reach the required carbon emission reductions for several reasons. Indeed, electric driven HP ease the use of renewable electricity production and can thus exclude the use of fossil-based energy resources for heating purposes. When smartly controlled, HP also enable the provision of energy flexibility services. In this context, new HP control strategies are investigated [1,2]. Though, to fairly compare smart and traditional control strategies, an accurate HP model is required. Several authors already indicated the necessity to precisely represent the real HP behaviour. In their research, Evens and Arteconi [3], investigated the effects of neglecting/incorporating the internal control strategies of HP such as timing constraints, compressor control, pump control, back-up heater (BUH) control etc. By gradually increasing the HP modelling complexity, the authors showed a changing operational behaviour which was caused by different control blocks. With most effects visible in the short-term, the authors also showed an affected energy flexibility. Moreover, Clauß and Georges [4] investigated the modelling complexity of HP and showed that for short-term analysis, such as demand response, a precise HP model is required.

Though, an accurate short-term behaviour HP model is novel and requires manufacturer information about internal control strategies. To better understand and represent its real behaviour, HP models should be validated and calibrated against experimental results. As field trials require a physical

building and are hard to compare due to changing boundary conditions, hardware-in-the-loop (HIL) experiments enable the optimal use of both software and hardware. The building and its heat emission system can be kept in simulations, while a real HP can be coupled to an experimental test bench. Within this framework, several studies already proved the added value of HIL experiments. In their study, Blervaque et al. [5] compared four different modelling approaches for air/air HP and showed modelling difficulties due to the amount of parameters when calibrating. In [6], El-Baz et al. investigated the energy performance of brine/water HP and developed a Modelica model to represent the dynamic HP behaviour which showed deviations up to 3 % and 4 % for the produced heat and electricity consumption, respectively.

In addition, Ruiz-Calvo et al. [7] developed TRNSYS models to represent a Mediterranean building equipped with a water/water HP and for which they also compared HP models to field measurements. Furthermore, Conti et al. [8] compared the energy performance of an air/water HP in a HIL experiment to simulations based on manufacturer datasheets. They concluded that the transient behaviour of the real HP reduced its energy performance. Moreover, Péan et al. [9] experimentally investigated Model Predictive Control (MPC) strategies for HP and clearly showed practical bottlenecks when coupling the steady-state MPC controller to the real HP. They concluded that the dynamic HP operation differed from the scheduled plan of the MPC controller and proposed solutions to overcome these difficulties.

Insights in these modelling approaches and HIL experiments indicated that internal HP control strategies are mainly neglected or simplified. It could be seen that the pump control is generally replaced by constant flow rate provision or that on/off pump control was used. In addition, compressor control, timing constraints and BUH control are generally simplified. Furthermore, in some cases, the HP control decisions were used as inputs in simulation environments, e.g. using the measured compressor frequency as a model input. Although that such an approach is useful to predict the actual performance/status of the real HP, it cannot be used in a full simulation environment. Indeed, in those cases, the HP model should be complete by itself and it should well represent the operational behaviour.

The goal of this paper is twofold. In a first part, an experimental set-up will be presented, including the required measurements and communication set-up. In a second part, the HIL set-up was used to validate and to further improve a dynamic HP model, able to represent the operational behaviour of the HP. The validation work includes an analysis of both the energy consumption and short-term behaviour.

2. Research methods

This sections starts with a description of the HIL set-up and the required communication. As the test bench is used to validate a water/water HP model, the HP model parameters are shown and are based on a detailed analysis of the HP documentation. Hence, the HP model should well replicate the real HP behaviour. This section also presents HP model validation cycles. As results will show, deviations between the experiments and simulation model occurred and led to HP model improvements as will be further discussed within the Results section.

2.1 Hardware-in-the-loop set-up description

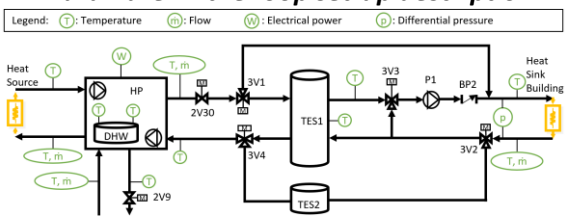

Fig. 1 – Hydraulic lay-out

Fig. 1 shows a hydraulic scheme of the HIL set-up with a reversible water/water HP, including corresponding measurements. The HP in place is a Daikin type EGSAX06DA9W with a nominal thermal power of 7.98 kW at B0/W35 according EN 14511 [10]. The HP also has a 180 l integrated domestic hot water (DHW) tank and is equipped with a 3 kW BUH. Tab. 1 provides more specifications of the measuring devices and the relative error at nominal conditions for the coefficient of performance (COP) is 1.661 %.

Tab. 1 – Specifications of measuring devices

Measurement	Specifications and accuracy
Temperature	Four-wire PT100 : 1/10 DIN Class B, except two DIN Class A sensors within the DHW TES
Flow	Electromagnetic: ± 0.2171 %
Differential pressure	± 0.055 % for a measuring span of 100 kPa
Electrical power	EN 50470-3 Class B: ± 1 %

Both the heat source and building load are emulated by heat exchangers for which a supply water setpoint can be set. The setpoint is reached by mixing cold and hot water from the laboratory with 3-way valves. Valve 2V9 emulates DHW draw-offs, while cold water is supplied by the community water grid. For space heating/space cooling (SH/SC), different hydraulic configurations can be realised, by either bypassing thermal energy storage (TES) TES1 via TES2 or by using TES1 in parallel or even partially bypassing TES1. Three-way valves and back-pressure valves (BP) enable the remote change of the hydraulic set-up. For TES1, a 200 l or 750 l storage can be tested, while TES2 is sized at 25 l to reach a minimum water volume for sufficient thermal inertia in case of directly coupling the HP to the virtual building as required by the manufacturer. Thermal stratification in TES1 is measured by 2 or 4 temperature sensors for the 200 l or 750 l TES, respectively. When TES1 is

used between the HP and virtual building, the flow rate of pump P1 can be set via an analogue input signal. For this paper, TES2 was used, while TES1 was bypassed. The HP is also equipped with both an evaporator and condenser pump which are internally controlled by the HP. Valve 2V30 can be used to throttle the internal condenser pump as its flow rate cannot be controlled by the user. Finally, the set-up allows to change the measured outdoor temperature by the HP as its outdoor temperature sensor was replaced by a potentiometer.

2.2 Hardware-in-the-loop communication

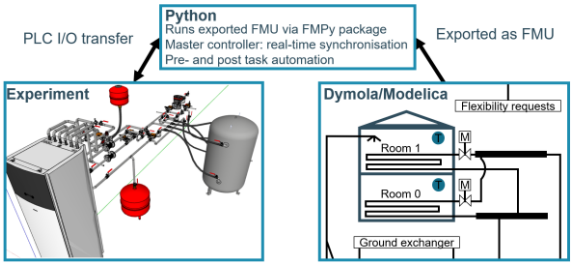

Fig. 2 – Communication set-up of the HIL-experiment

Fig. 2 shows the communication set-up between the simulation and experiment. A PLC is used to retrieve measurements from and send setpoints to the experiment at time steps of 15 seconds. The communication interval should be small enough to correctly represent the real HP behaviour and to provide correct inputs for both the experimental and simulation environment [11,12]. Furthermore, A Modelica model is translated into a FMU-file (Functional Mock-up Unit) and imported in Python via the FMPy package [13]. Python acts as a master controller to maintain the real-time synchronisation.

The HP is also equipped with a Modbus-interface to remotely communicate both the setpoints and measurements within the HP system. The Modbus interface allows the setting of the condenser leaving water temperature in both SH and SC mode, the DHW reheating temperature and the (de)activation of SH, SC, DHW, DHW booster and quiet working mode. Internal HP measurements are temperatures at the condenser inlet and outlet, temperature after the back-up heater, DHW tank temperature, liquified refrigerant temperature and condenser pump flow rate. In addition, fault codes and the status of the compressor, circulation pump, legionella protection service, booster, three-way valve and operational mode can be read out. Though, it should be noted that the accuracy of the measurements within the HP itself is not known due to a lack of documentation. Hence, measurements outside the HP are preferred.

The HP also has energy flexibility interfaces such as a preferred kWh contact, a SG-ready interface [14] and digital inputs to limit its power consumption.

2.2 Heat pump model

Modelling the HP internal control strategies requires manufacturer information and is not error prone. A preliminary work [3] investigated the modelling approaches for short- and long-term HP behaviour. The HP model in the current paper starts from the most accurate model in the preliminary work. The modelling parameters are based on the HP manufacturer documentation and provide the best estimate. The model includes performance data for both part- and full-load conditions, minimum compressor on/off-times, minimum compressor modulation, DHW timing constraints, anti-legionella cycles for the DHW disinfection, BUH control, proportional-integral (PI) condenser pump control. Tab. 2 summarises the HP model start parameters.

Tab. 2 – Overview heat pump modelling data

Start parameter	Value
Minimum compressor speed	Condenser outlet temperature dependent
Performance data	Tables with thermal and electrical power at 30 %, 50 %, 70 %, 90 % and 100 %
Compressor off-temperature	Setpoint + 2 °C
Compressor on-temperature	Setpoint – 2 °C
Compressor cycles	Maximum 6 per hour
BUH control	Discrete steps of 1 kW and only activated after compressor switch-off at a 53 °C DHW TES temperature during anti-legionella cycles
DHW on-time	Minimum one minute, while the maximum time is weather dependent, unless a fixed maximum time of 125' for anti-legionella cycles
DHW off-time	Minimum 30 minutes
DHW control	Cycle starts if the DHW TES temperature drops below 42 °C and cycle stops at 47 °C
Anti-legionella cycle control	Keep DHW temperature at 60 °C for at least 40 minutes with a maximum anti-legionella cycle duration of 4 hours before forcing an error if not accomplished
Condenser pump control	PI-controlled to maintain a 5 °C temperature difference between HP outlet and inlet, with a minimum flow rate of 12 l/min, with pump curves
Evaporator pump control	Continuous fixed speed operation with pump curves

2.3 Model validation with predefined cycles

Comparing the short-term behaviour of a real HP

system and a HP simulation model by directly coupling it to a building heat emission system can cause validation issues. Indeed, the mutual influence of the HP and building prevent an easy distinction of the different modelling parameters of the HP model. In addition, the dynamic behaviour of heat emission systems such as underfloor heating systems complicate a model validation and possibly require post-corrective measures. Therefore, it was chosen to validate the HP model according to a predefined load profile which was artificially constructed, both for SH and DHW provision. During all cycles, the evaporator inlet temperature setpoint was fixed at 15 °C. The minimum return temperature from the SH load was set to 20 °C to prevent unlimited SH load extraction during DHW mode. Indeed, during DHW charging cycles, the HP is not providing SH services.

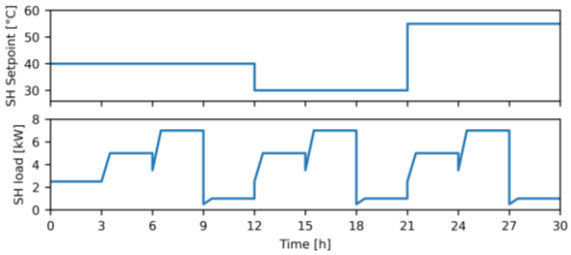

Fig. 3 – SH Cycle 1 with three hours of preconditioning

For SH purposes, three different supply water temperature setpoints were used, namely 30 °C, 40 °C and 55 °C. For each of those temperature setpoints, three thermal loads were tested and set at 1 kW, 5 kW and 7 kW. Fig. 3 shows the SH load profile in which a preconditioning period of three hours was foreseen to start the system. Each setpoint was maintained for three hours in which the SH load linearly increased from 50 % to 100 % of the required load in the first 30 minutes to assure a stable operation of the experimental facility and HP. Except for the preconditioning period, this SH cycle was executed two times to provide sufficient data for each setpoint as DHW provision was also activated and influenced the operational behaviour. This cycle was mainly used to validate the controller stability for the compressor and circulation pumps.

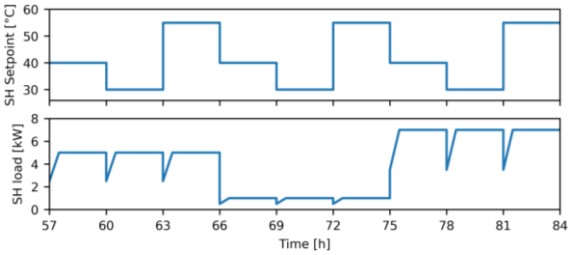

Fig. 4 – SH Cycle 2

A second cycle, as shown in Fig. 4, focusses on the HP dynamics during changing SH temperature setpoints and loads. This cycle was executed only once, but shows similarity to the first SH cycle. The two cycles only differ in the order of firstly changing the SH thermal load and SH temperature setpoint afterwards for Cycle 1 and firstly changing the SH temperature setpoint and then the load for Cycle 2.

A DHW draw-off profile was derived from a profile generation tool of Jordan et al. [15]. Four different flow rates of 5 l/min, 7 l/min, 8 l/min and 12 l/min were used for fixed time slots of 1', 1', 5' and 10', respectively. Combining the extracted flow rates, an average daily draw-off volume of 242 l was reached. The experiment also included an anti-legionella cycle, which enabled the BUH controller validation. Lastly, to validate the weather-dependency of the DHW timing constraints, tests were performed for two outdoor temperatures, namely 0 °C and 8 °C.

3. Results

This section presents the HP model validation and contains HP model improvements. Prior to the model validation, the pressure losses and water content of the experimental facility were implemented in the simulation model. On the level of the evaporator, a maximum flow rate of 32.4 l/min was reached, while 18 l/min was measured for the condenser water flow rate during SH mode. By using the HP manufacturer pump curves, pressure losses were implemented. Due to insufficient technical data, the pressure losses of the DHW heating spiral could not be determined in advance and were thus kept at a default value.

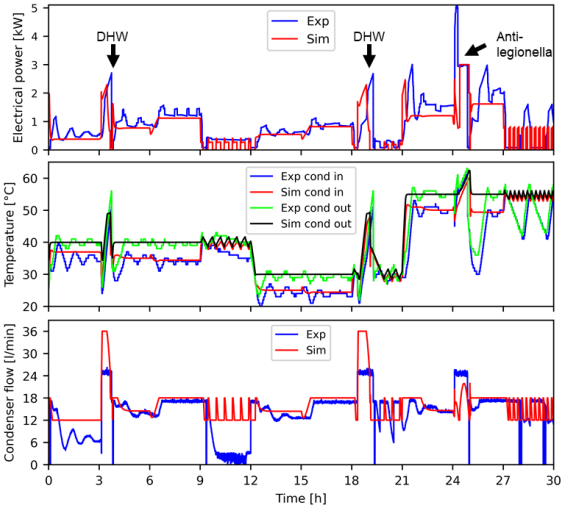

Fig. 5 – SH Cycle 1: electrical power, condenser water temperatures and water flow rate - original

Fig. 5 compares the experimental (Exp) and simulated (Sim) results of the original HP model for the electrical power, condenser water inlet (cond in) and outlet (cond out) temperatures and the condenser water flow rate during SH Cycle 1. It shows reasonable agreements when considering the condenser inlet and outlet temperatures, while the condenser water flow rate and the overall HP power consumption show higher variations. In addition, analysing the short-term behaviour, the experiments showed more variability around the temperature setpoint, while the simulation results showed a more stable behaviour. The simulated HP model was also able to faster reach the temperature setpoint.

The aforementioned differences can be explained by the HP modelling approach. Firstly, the modelled compressor was not equipped with a proportional

integral derivative (PID) controller, but the model used a modulation controller with the performance curves to determine the required compressor speed. Such an approach causes the compressor to take an immediate action as soon as a difference between the measured and required setpoint is measured. In addition, the minimum thermal capacity of the experimental HP was also lower compared to the HP model. This can be seen in Fig. 5 from hour 9 till hour 12 in which the real HP was able to remain activated, while the HP model performed cycling behaviour.

Secondly, the condenser pump control is also different. The modelled minimum condenser flow rate of 12 l/min was only required in space cooling mode and not during space heating. Further experimental analysis showed a minimum flow rate of 2.8 – 3.2 l/min. In addition, the condenser pump control in SH mode differed from DHW mode, while the HP model assumed a control approach which tries to keep 5 °C temperature difference between HP inlet and outlet water, both for SH and DHW mode. Such an approach was correct for SH mode, while the HP maintained a fixed water flow rate of 25 l/min during DHW mode. Comparison with experimental results also showed the inability of the modelled controller to quickly react on temperature changes.

Thirdly, the simulated electricity consumption is mainly lower than the experimental results. This is due to the use of the performance maps. These maps should already incorporate the consumption of additional equipment such as the evaporator pump, condenser pump and control logic, though for only a small part. Indeed, the additional consumption due to head losses and control logic should only refer to the losses caused by the device itself [16]. Hence, measurements according EN 14511 [17] neglect the head losses of ground loops and SH circuits.

Fourthly, the HP cycles during too low compressor modulation speeds are different. While the HP model used a hysteresis of +2/-2 °C around the setpoint temperature, the real controller uses both the supply and return temperature in an AND-function to determine the compressor off-signal. Analysis showed that the compressor remained on as long as the supply temperature did not increase 3 °C above the temperature setpoint and as long as the return temperature did not reach the supply temperature setpoint. An exception is made for when the supply temperature reaches a temperature 5 °C higher than the setpoint temperature. In those cases, the return temperature is not incorporated due to safety constraints. Such an approach allows a more stabilised compressor operation and prevents excessive compressor cycles as both the supply and return temperature should reach a certain threshold. The lower hysteresis limit of a supply temperature 2 °C below the supply temperature setpoint was still correctly modelled. Moreover, the compressor off-time was also 2' shorter compared to the HP model.
Differences could also be seen during anti-legionella cycles. According the operation ranges of the BUH and compressor, the BUH only works at DHW temperatures above 53 °C. During the experiments, it could be seen that within anti-legionella cycles, the BUH can simultaneously work with the compressor. Both elements are initially activated, while the compressor turned off at a DHW temperature of 53 °C. The simultaneous operation of the compressor and BUH caused a faster anti-legionella cycle, but also decreased the efficiency due to the lower efficiency of the electrical resistance. In addition, the BUH power was not exactly 3 kW but slightly lower, even if measuring errors were considered.

The HP model also showed dependency on the measuring height of the DHW TES temperature sensor, the position of the heating spiral and the insulation thickness. With a ten layer-stratified DHW TES model, it was concluded that positioning the sensor in the third layer with a hot water spiral ranging from a height of 10 % – 75 % and a smaller insulation thickness showed better agreement with the experimental results. In contrast with the simulations, the experimental DHW temperature has a resolution of 1 °C due to the HP Modbus module.

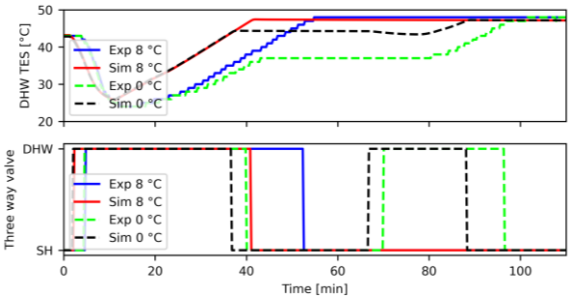

Fig. 6 – Maximum DHW cycle time weather dependency

Fig. 6 shows the comparison of a DHW charging cycle for two different outdoor temperatures, namely 0 °C and 8 °C. It can be seen that the DHW TES was not completely charged within the maximum DHW cycle time at an outdoor temperature of 0 °C. Hence, a second DHW cycle was necessary after the minimum DHW off-time. In contrast, the maximum DHW cycle time was not reached for an outdoor temperature of 8 °C. Results also showed that the maximum time for anti-legionella cycles was not weather-dependent.

In addition, during DHW cycles, the measured supply temperature differed from the simulation results. Within the model, it was assumed that the condenser supply temperature was limited to 55 °C as stated by the HP manufacturer. Experiments indicated that the compressor was able to provide condenser temperatures until 60 °C. Furthermore, the HP model showed a decreasing modulation speed towards the DHW charging cycle end, while the experimental HP remained close to full-load conditions. This can be explained by the HP model in which a supply water setpoint of 2 °C higher than the DHW temperature setpoint was modelled, while it is assumed that the experimental HP has a fixed compressor setpoint temperature of 60 °C to fasten the DHW cycles.

Fig. 7 shows an improved similarity between the

experimental and simulated results after model improvement of the aforementioned differences. Although a better profile agreement, differences still exist. Indeed, larger variations between experiment and model occurred during SH temperature setpoints of 55 °C, for which Fig. 8 shows more details. During the shown time slot, the SH supply setpoint increased from 40 °C to 55 °C, while SH load variations are also indicated within the figure. The shown temperatures are the temperatures within the HP system and thus dependent on the provision of SH or DHW services. Moreover, it can be seen that an anti-legionella cycle occurred from hour 24 to hour 25. A reasonable good match can be seen for SH loads above the minimum thermal capacity.

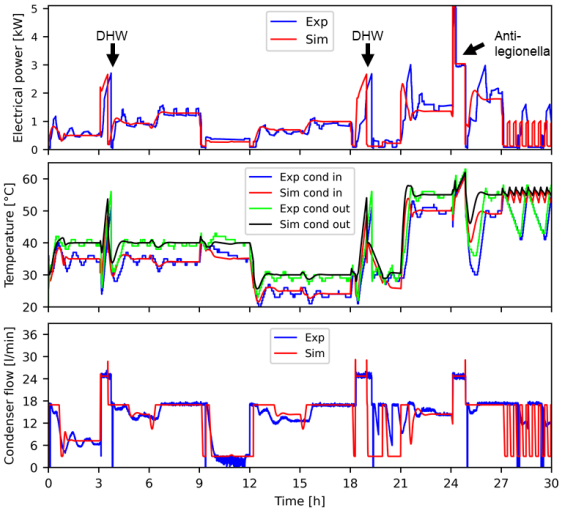

Fig. 7 – SH Cycle 1: electrical power, condenser water temperatures and water flow rate – adapted

Though, for low SH loads, the real HP was not able to closely follow the temperature setpoint. Indeed, when the compressor off-trigger signal is reached, the real HP remains off for a long time, while the simulated HP was able to remain close to the requested SH temperature. Such a behaviour only appeared during low SH loads accompanied by high temperature setpoints. Further experimental tests at other, but also high SH temperature setpoints, showed equal behaviour. As shown in Fig. 8, the compressor was only reactivated as soon as the return temperature dropped below 45 °C and it could be seen that this remained independent from the supply temperature setpoint. This control approach is also in contrast with the approach for lower SH temperature setpoints as already showed. It could be explained by a possible internal control strategy from the HP manufacturer to limit the number of compressor cycles during low SH loads at high SH supply temperatures. Further experimental tests will determine the exact point for which the internal control strategy is changed. Fig. 8 also indicates a compressor switch-off after a 2' on-time, while the setpoint was not reached. Analysis showed that during those moments, the liquified refrigerant temperature was not equal to or above the return temperature at the condenser side and caused the compressor to switch off. In those cases, the HP controller assumed that the compressor was not heating up, but cooling down the condenser. Hence, it switched off the compressor, while for those cases, it could also be seen that the minimum compressor off-time was reduced from 6' to 4.5'. Finally, as the HP model is based on performance maps, including a refrigerant temperature-dependency is difficult.

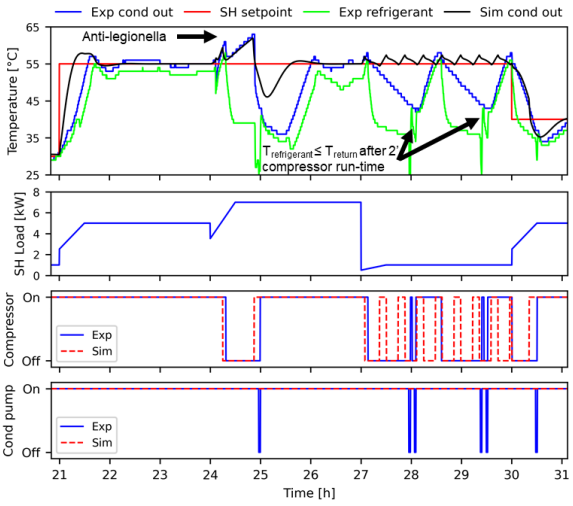

Fig. 8 – Cycling behaviour at 55 °C SH supply setpoints

Analysis of DHW cycles also showed a consistent compressor switch-off after a DHW cycle, even with a SH setpoint of 55 °C. As HP mainly provide low SH temperatures to e.g. an underfloor heating system, the switch-off signal can be caused by a HP safety control strategy. Indeed, such a strategy prevents too high supply temperatures fed into the SH system.

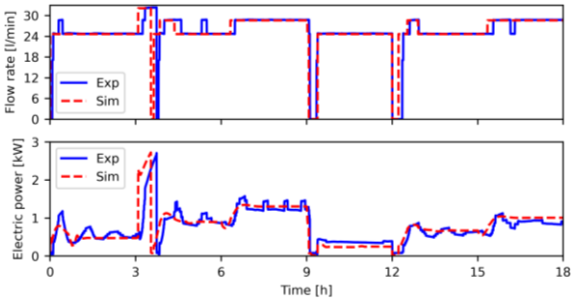

Fig. 9 – Evaporator pump control

The condenser pump control also differed, while a continuous operation was expected due the HP settings in place. If the compressor activation was triggered and if the condenser outlet was more than three degrees higher than the liquified refrigerant temperature, then the pump switched off for two minutes. Afterwards, both the pump and compressor were simultaneously activated. At the level of the evaporator, the evaporator pump went off along with compressor, while it switched on two minutes prior to the compressor activation. Four evaporator flow rates were detected and showed a dependency on the compressor speed. Pump speeds of 76 %, 89 % and 100 % were found for compressor speeds below 45 %, 45 – 75 % and 75 – 100 %, respectively. When the evaporator pump started two minutes in advance to the compressor, the pump speed was 53 %. While such a hypothesis should be further verified with more experiments, Fig. 9 shows similarities between

the hypothesis and experiment. It should be noticed that the compressor speed was estimated from the HP model as it was not possible to read out the compressor speed from the real HP.

Tab. 3 – Full cycle duration analysis (84 hours) after model improvement at an outdoor temperature of 8 °C

Overall indicator	HIL	Simulation
Evaporator energy (kWh)	382.2	300.9 (- 21.3 %)
SH energy (kWh)	327.7	329.3 (+ 0.5 %)
DHW thermal energy (kWh)	26.9	31.1 (+ 15.6 %)
Electrical energy (kWh)	77.5	76.9 (- 0.8 %)
Total DHW draw-off volume (l)	829.5	799.7 (- 3.6 %)
Compressor cycles	39	41 (+ 5.1 %)
DHW cycles	6	6 (0 %)

Tab. 3 shows performance indicators for comparing the simulated to the experimental results over a full cycle duration of 84 hours at an outdoor temperature of 8 °C. While small variations exist for the majority of the indicators, larger deviations were found at the evaporator level and DHW provision. Differences within DHW provision can be explained by the time delay and PI-control of the experimental DHW draw-off valve. Before reaching a stable flow rate within +/- 10 % of the setpoint required on average 30 – 45 seconds. Results also showed larger deviations for small flow rates up to two times the required flow rate due to the controller overshoot and also, due to the pressure difference over the DHW valve. Hence, the extraction of small flow rates for short time slots can be found as the main reason for those differences. Hence, for future experimental testing, a DHW flow accumulator will be tested to close the valve when the required draw-off volume is reached. The experimental DHW inlet temperature was also mainly warmer compared to a modelled temperature of 10 °C. Indeed, during periods without DHW draw-offs, the temperature of the piping materials and water converged to the environmental temperature of 22 °C, while during draw-off periods of several minutes, a temperature of 10 °C was measured. Using the experimental inlet temperature within the simulation, decreased the DHW thermal energy from 31.1 kWh to 25.5 kWh, which is closer to the experimentally measured DHW energy of 26.9 kWh.

At the evaporator level, two main differences were seen. While the condenser heat exchanger followed the required temperature setpoint within +/- 0.25 °C, the evaporator heat exchanger showed larger variations of mainly +/- 0.75 °C. Reasons can be found in the modulation control of the real HP which increased stepwise. These steps caused sudden temperature drops in the evaporator return temperature for which the heat exchanger could not directly react due to its system inertia. Moreover, the off-state of the evaporator pump within the HP caused the PI controller of the heat exchanger to saturate as it did not detect a change of the measured temperature. Hence, the heat exchanger temperature went to one of the two supply temperatures of the laboratory. Though, analysis showed that including these temperature variations within the simulations did not cause major improvements as the HP model mainly extracted less evaporator power which caused a smaller simulated temperature difference between evaporator inlet and outlet. As the HP model is based on performance maps with the thermal condenser (*Qcond*) and electrical power (*Pelec*), reasons can be found in the determination of the evaporator power (*Qevap*) as shown in equation (1).

$$Qevap = Qcond - Pelec \quad (1)$$

Such an approach assumes an ideal conversion of all electrical energy into useful thermal energy, while a part is also preserved for supplying the control logic and for both the evaporator and condenser pump. Therefore, a recalculation factor within the HP model should separate the electrical power from the performance maps into two parts, namely (1) a compressor power which is converted into thermal energy and (2) an auxiliary power supply. While such an approach should be further verified, it remains unlikely to completely solve the evaporator energy difference. Indeed, the energy difference is 81.3 kWh, while the overall electricity consumption within the experiment was only 77.5 kWh. Hence, it can be stated that performance maps do not allow an accurate determination of the extracted evaporator power. Further experiments will also evaluate the evaporator power extraction on both the primary and secondary side of the heat exchangers.

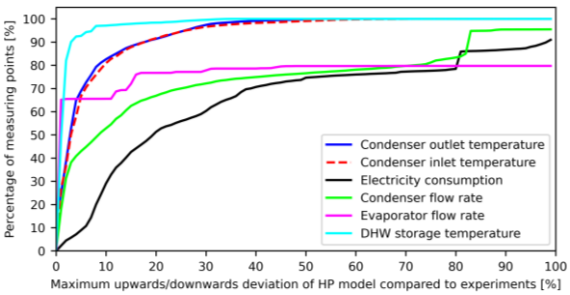

Fig. 10 – HP model agreement to experimental results

Finally, Fig. 10 shows the agreement of several HP model variables to the experimental results. The curves can be interpreted as duration curves which contain all data points with time steps of 15 seconds. For a certain percentage of the measured points on the vertical axis, the horizontal axis provides the maximum deviation percentage of the HP model, e.g. a maximum deviation of +/- 10 % for 83 % of the data points of the condenser outlet temperature. It can be seen that DHW and condenser temperatures show good agreement, while the pump control and especially the electricity consumption show the necessity for a future calibration work with more experimental data as previously explained.

4. Conclusions

This paper presented a hardware-in-the-loop test bench to develop new control strategies for energy flexibility provision with water/water heat pumps. It showed a thorough presentation of the set-up, the communication requirements, the possible hydraulic configurations and a description of the measuring equipment, for which a relative measuring error of 1.661 % on the coefficient of performance was determined. In a second part, the test bench was used to validate a water/water heat pump model. As the model not only includes the performance maps, but also the internal control strategies such as timing constraints, compressor control and pump control, both the overall energy consumption and short-term behaviour were analysed. An overall energy analysis showed that direct usage of the performance maps underrated the energy consumption due to the neglection of the heat pump auxiliary equipment. Inclusion of those elements, showed a closer match, while deviations remained for the evaporator energy, electricity consumption and domestic hot water. A short-term behaviour analysis also showed the necessity for heat pump model improvements as the experimental results differed from the modelling assumptions, which were derived from the heat pump documentation. Model improvements by using new timing constraints and modulation controllers showed better agreement. Though, the experiments showed unexpected behaviour for the combination of low space heating loads and high temperatures for which the heat pump was not able to closely follow the temperature setpoint. Hence, it was shown that an accurate heat pump model is required to represent the real heat pump behaviour, especially when analysing energy flexibility. It was shown that modelling the real heat pump behaviour only based on heat pump manufacturer documentation is not sufficient. A future work will present a calibrated heat pump model and the development of control strategies for energy flexibility with heat pumps.

5. Acknowledgement

This research work was funded by the Internal Funds KU Leuven. We thank Daikin for providing part-load data for the heat pump EGSAX06D9W.

6. References

[1] Hogeling J, Corgnati S, Dziergwa A, Ceyhan I. The REHVA European HVAC Journal. Vol 54, Issue 2. 2021;58(4):76.

[2] Arteconi A, Hewitt NJ, Polonara F. Domestic demand-side management (DSM): Role of heat pumps and thermal energy storage (TES) systems. Appl Therm Eng. 2013;51(1–2):155–65.

[3] Evens M, Arteconi A. Influence of Internal Control Simplifications in Heat Pump System Modelling for Energy Flexibility Evaluations. In: Proceedings of Building Simulation 2021: 17th Conference of IBPSA. IBPSA; 2021.

[4] Clauß J, Georges L. Model complexity of heat pump systems to investigate the building energy flexibility and guidelines for model implementation. Appl Energy. 2019;255(May):113847.

[5] Blervaque H, Stabat P, Filfli S, Schumann M, Marchio D. Variable-speed air-to-air heat pump modelling approaches for building energy simulation and comparison with experimental data. J Build Perform Simul. 2016;9(2):210–25.

[6] El-Baz W, Tzscheutschler P, Wagner U. Experimental study and modeling of ground-source heat pumps with combi-storage in buildings. Energies. 2018;11(5).

[7] Ruiz-Calvo F, Montagud C, Cazorla-Marín A, Corberán JM. Development and experimental validation of a TRNSYS dynamic tool for design and energy optimization of ground source heat pump systems. Energies. 2017;10(10).

[8] Conti P, Bartoli C, Franco A, Testi D. Experimental analysis of an air heat pump for heating service using a "hardware-in-the-loop" system. Energies. 2020;13(17).

[9] Pean T, Costa-Castello R, Fuentes E, Salom J. Experimental Testing of Variable Speed Heat Pump Control Strategies for Enhancing Energy Flexibility in Buildings. IEEE Access. 2019;7:37071–87.

[10] Technical Data EGSAH/X series Daikin. Oostende; 2020.

[11] Zottl A, Nordman R, Coevoet M, Riviere P, Benou A, Riederer P. D4.1/D2.3 Guideline for heat pump field measurements for hydronic heating systems. 2011;1–33.

[12] Haller MY, Haberl R, Persson T, Bales C, Kovacs P, Chèze D, et al. Dynamic whole system testing of combined renewable heating systems - The current state of the art. Energy Build. 2013;66:667–77.

[13] FMPy. Dassault Systèmes.

[14] Bundesverband Wärmepumpe e.V. (bwp). SG Ready-label.

[15] Jordan U, Vajen K, Braas H. DHWcalc: Tool for the Generation of Domestic Hot Water Profiles on a Statistical Basis (version 2.02b). 2017;10(March):1–14.

[16] Klein B. Independent testing of heat pumps is needed for reliable COP. REHVA J. 2012;(October):15–8.

[17] EN 14511-3:2018 - Air conditioners, liquid chilling packages and heat pumps for space heating and cooling and process chillers, with electrically driven compressors - Part 3: Test methods. 2018.

Data Statement

The datasets generated during and/or analysed during the current study are available in the Clima2022 repository, . https://github.com/Maaeve/Clima2022.